Towards an understanding of thallium isotope fractionation during adsorption to manganese oxides

Sune G. Nielsen[1,2*], Laura E. Wasylenki[3], Mark Rehkämper[4], Caroline L. Peacock[5] ,

Zichen Xue[4] and Ellen M. Moon[6♀]

[1]Department of Geology and Geophysics, Woods Hole Oceanographic Institution, Woods Hole, 02543

MA, USA

[2]Department of Earth Science, University of Oxford, Parks Road, OX1 3AE, Oxford, UK

[3]Department of Geological Sciences, Indiana University, Bloomington, IN, USA

[4]Department of Earth Science and Engineering, Imperial College, London SW7 2AZ, UK

[5]School of Earth & Environment, University of Leeds, Leeds LS2 9JT, UK

[6]University of Southampton, School of Ocean and Earth Science, National Oceanography Centre

Southampton, SO14 3ZH, UK

♀Current address: ANSTO Minerals, Australian Nuclear Science and Technology Organisation,

Locked Bag 2001, Kirrawee D.C., NSW 2234, Australia

* corresponding author: snielsen@whoi.edu

20   **Abstract** - We have conducted the first study of Tl isotope fractionation during sorption

21   of aqueous Tl(I) onto the manganese oxide hexagonal birnessite. The experiments had

22   different initial Tl concentrations, amounts of birnessite, experimental durations, and

23   temperatures, but all of them exhibit heavy Tl isotope compositions for the sorbed Tl

24   compared with the solution, which is consistent with the direction of isotope fractionation

25   observed between seawater and natural ferromanganese sediments. However, the magnitude

26   of fractionation in all experiments ($\alpha \approx$ 1.0002 to 1.0015, where $\alpha = {}^{205}Tl/{}^{203}Tl_{solid}$ /

27    ${}^{205}Tl/{}^{203}Tl_{liq}$) is smaller than observed between seawater and natural sediments ($\alpha \approx$ 1.0019 to

28   1.0021; Rehkämper et al., 2002, *Earth. Plan. Sci. Lett.* 197, 65-81). The experimental results

29   display a strong correlation between the concentration of Tl in the resulting Tl-sorbed

30   birnessite and the magnitude of fractionation. This correlation is best explained by sorption of

31   Tl to two sites on birnessite, one with large isotope fractionation and one with little or no

32   isotope fractionation. Previous work (Peacock and Moon, 2012, *Geochim. Cosmochim. Acta*

33   84, 297-313) indicates that Tl in natural ferromanganese sediments is oxidized to Tl(III) and

34   adsorbed over Mn vacancy sites in the phyllomanganate sheets of birnessite, and we

35   hypothesize that this site is strongly fractionated from Tl in solution due to the change in

36   oxidation state from aqueous Tl(I). In most experiments, which have orders of magnitude

37   more Tl associated with the solid than in nature, these vacancy sites are probably fully

38   saturated, so various amounts of additional Tl are likely sorbed to either edge sites on the

39   birnessite or triclinic birnessite formed through oxidative ripening of the hexagonal starting

40   material, with unknown oxidation state and little or no isotopic fractionation. Thus each

41   experiment displays isotopic fractionation governed by the proportions of Tl in the

42   fractionated and slightly fractionated sites, and those proportions are controlled by how much

43   total Tl is sorbed per unit of birnessite. In the experiments with the lowest initial Tl

44   concentrations in solution (~0.15-0.4 µg/g) and the lowest concentrations of Tl in the resulting

45 Tl-sorbed birnessite (≤17 μg Tl/mg birnessite), we observed the largest isotopic

46 fractionations, and fractionation is inversely proportional to the initial aqueous Tl

47 concentration. Again, this correlation can be explained by the simultaneous occupation of two

48 different sorption sites; vacancy sites that carry isotopically fractionated Tl and a second site

49 carrying slightly fractionated Tl. The fractionation factors observed in nature exceed those in

50 the experiments likely because the Tl concentrations in seawater and in ferromanganese

51 sediments are three to four orders of magnitude lower than in our experiments, and therefore

52 the second slightly fractionated sorption site is not significantly utilized. Temperature (6°C to

53 40°C) and experimental duration (3 min to 72 hr) appear to have little or no effects on isotope

54 behaviour in this system.

55

1. Introduction

Ferromanganese (Fe-Mn) marine sediments are commonly used in marine geochemistry to study changes in ocean circulation and variations in the marine source and sink fluxes of the respective elements (Frank, 2002). Slow accumulation and enrichment in many metals allow these rocks to record the elemental and isotopic evolution of the seawater from which they precipitate, and such records are of importance to paleoclimate studies. Traditionally, the focus has been on interpreting past distribution of radiogenic Nd, Hf, Os, and Pb isotope compositions in the oceans. With the advent of MC-ICPMS (multiple collector inductively coupled plasma mass spectrometry), a number of researchers have recently analyzed Fe-Mn crusts and nodules to obtain stable isotope records for metals, including Fe, Zn, Mo, Cd and Tl (Barling et al., 2001; Horner et al., 2010; Levasseur et al., 2004; Maréchal et al., 2000; Rehkämper et al., 2004; Schmitt et al., 2009; Siebert et al., 2003).

The interpretation of data obtained for such "unconventional" isotope systems is less straightforward, as they may record either variability in the isotope composition of seawater or changes in the conditions that govern incorporation of the elements into the Fe-Mn mineral assemblages. In order to develop paleoceanographic applications of such records, it is therefore important to obtain (i) a detailed characterization of how specific elements are sorbed by Fe-Mn minerals and (ii) a quantitative and mechanistic understanding of any isotopic fractionation that occurs during this process. This study presents the results of experimental work that was carried out to investigate the sorption of the element thallium (Tl) onto marine Fe-Mn deposits. Such studies are of general interest because temporal shifts in the Tl isotope composition of seawater, as recorded by Fe-Mn crusts, may provide new constraints on past changes in environmental conditions and the Earth's carbon cycle, and their impact on global climate (Baker et al., 2009; Nielsen et al., 2009a; Rehkämper et al., 2004).

Here, we conduct the first investigation aimed at understanding the Tl isotope fractionation observed between seawater and Fe-Mn deposits. Thallium in Fe-Mn deposits is strongly associated with the Mn oxide mineral birnessite (Koschinsky and Hein, 2003; Peacock and Moon, 2012). In addition, XANES and EXAFS studies of Tl sorbed onto birnessite (Bidoglio et al., 1993; Peacock and Moon, 2012) have shown that this process most likely occurs in three steps (Peacock and Moon, 2012). Firstly, monovalent Tl is attracted to the mineral surface as a loosely bound outer-sphere complex. This is followed by surface oxidation to Tl(III) and adsorption as an inner-sphere complex at Mn octahedral vacancy sites present in the phyllomanganate sheets of the birnessite. Observation of this process is an important result because theoretical calculations have previously predicted that equilibrium between the two naturally occurring oxidation states of Tl (*in vacuo*) can generate the large isotope fractionation observed between seawater and Fe-Mn crusts (Schauble, 2007). As such, Peacock and Moon (2012) propose a sorption-oxidation-fractionation mechanism to explain the Tl enrichment and isotope fractionation observed in real marine ferromanganese crusts.

To explore whether the mechanism proposed for Tl sorption to birnessite is responsible for natural Tl isotope fractionation we have performed several series of experiments in which we sorbed dissolved Tl(I) onto birnessite. We investigate the Tl isotope effects occurring during the sorption process as a function of time and temperature and for different abundances of sorbed Tl. While the results of these experiments do not exactly reproduce the isotope effects observed in nature, we believe that the outcomes present important clues to the processes behind Tl isotope fractionation during sorption onto Fe-Mn deposits. In conjunction with recently published theoretical aspects of Tl stable isotope fractionation (Schauble, 2007) we employ our experimental results to develop a consistent theory outlining the principal mechanism that likely causes Tl isotope fractionation in marine sediments.

106

2. Background

2.1. Geochemistry of thallium

The geochemistry of Tl has been the subject of a number of older and more recent publications. In the silicate Earth, Tl is a highly incompatible trace element that is concentrated in K-bearing phases (Heinrichs et al., 1980; Shaw, 1952; Wedepohl, 1974), because it occurs primarily in the form of Tl^+, which is similar in size to the large monovalent cations K^+, Rb^+ and Cs^+. However, unlike the alkali metals, Tl also exhibits chalcophile behaviour in the presence of sulphide melts and S-rich (hydrothermal) fluids (Heinrichs et al., 1980; McGoldrick et al., 1979). A few studies furthermore identified significant enrichments of Tl in volcanic plumes, as Tl is significantly more volatile in volcanic systems than the alkali elements (Gauthier and Le Cloarec, 1998; Hinkley et al., 1994; Patterson and Settle, 1987).

Some aspects of the marine geochemistry of Tl are also similar to K and the heavier alkali elements. In seawater, dissolved Tl is generally thought to be monovalent, occurring in the form of Tl^+, $TlOH^0$ and $TlCl^0$ species (Byrne, 2002; Nielsen et al., 2009a), and it displays a nearly conservative distribution (Bruland, 1983; Flegal and Patterson, 1985). Thallium also appears to be rapidly cycled through marine organisms in the same manner as K (Flegal et al., 1986).

However, there are also important differences between Tl and the alkali metals in the oceanic realm. At about 20,000 yr, the marine residence time of dissolved Tl is significantly shorter than those of K and Rb (Bruland, 1983; Rehkämper and Nielsen, 2004). This difference in behaviour appears to be related to the greater reactivity of Tl toward scavenging by authigenic Fe-Mn oxyhydroxides, as evidenced by (i) the high Tl concentrations of ferromanganese deposits, with up to ~100 µg/g Tl (Fig. 1), and pelagic clays (Heinrichs et al.,

131   1980; Matthews and Riley, 1969; Rehkämper et al., 2004) and (ii) the observation that the

132   oceans (and to a lesser extent rivers) have Tl to alkali metal ratios that are lower than the

133   continental crust (Bruland, 1983; Nielsen et al., 2005; Rehkämper and Nielsen, 2004; Rudnick

134   and Gao, 2003). The strong affinity of Tl for Fe-Mn oxyhydroxide minerals appears to reflect

135   oxidation of dissolved seawater Tl(I) to Tl(III) on the active surfaces of the Fe-Mn

136   oxyhydroxides (Bidoglio et al., 1993; Peacock and Moon, 2012; Rehkämper et al., 2004;

137   Rehkämper et al., 2002).

138

139   **2.2. Thallium isotopes**

140   Thallium has two stable isotopes, ^{203}Tl and ^{205}Tl, and a number of studies have explored

141   natural isotope fractionations of Tl over the last 10 years. These investigations revealed stable

142   isotope variations in terrestrial samples spanning 35 ε^{205}Tl units, where

143        $\varepsilon^{205}\text{Tl}_{sample} = 10^4 \times (^{205}\text{Tl}/^{203}\text{Tl}_{sample} - ^{205}\text{Tl}/^{203}\text{Tl}_{NIST\ 997})/(^{205}\text{Tl}/^{203}\text{Tl}_{NIST\ 997})$ (1)

144   and NIST 997 is a standard reference material defined as ε^{205}Tl = 0 (Nielsen et al., 2006b;

145   Rehkämper et al., 2004; Rehkämper et al., 2002). This is a surprising result, as it shows that

146   Tl displays a similar magnitude of stable isotope variability as significantly lighter elements,

147   such as Fe, Zn, and Cd, despite a much smaller relative mass difference of less than 1%. The

148   Tl isotope variability is particularly pronounced in the marine environment. The Tl isotope

149   composition of open-ocean seawater, as determined from analyses of 8 samples from the

150   Atlantic, Pacific and Arctic Oceans, is ε^{205}Tl = -5.7 ± 0.4 (Nielsen et al., 2004; Nielsen et al.,

151   2006b; Rehkämper et al., 2002). This isotope composition is somewhat lighter than the

152   average composition of the Earth's continental crust and mantle, which are both characterized

153   by ε^{205}Tl = -2.0 ± 0.5 (Nielsen et al., 2007; Nielsen et al., 2006a; Nielsen et al., 2005). In

154   contrast, Tl-rich basalts from weathered upper ocean crust and Fe-Mn crusts are known to

155   have ε^{205}Tl values as low or as high as about -20 and +15, respectively (Nielsen et al., 2006b;

156   Rehkämper et al., 2002).

157   Of particular interest are the systematic Tl isotope relationships that were determined for

158   various marine Fe-Mn deposits (Fig. 1). Hydrogenetic Fe-Mn crusts are thought to precipitate

159   directly from seawater, and Tl data are available for the recent growth surfaces of 17 samples

160   from all major ocean basins. These analyses revealed Tl isotope compositions that do not

161   correlate with radiogenic isotope data and display only a narrow range of ε^{205}Tl values

162   (between of +10 and +14) with a mean result of ε^{205}Tl = 12.8 $\pm$ 1.2 (1sd, n = 17) (Rehkämper

163   et al., 2002). The Fe-Mn crusts thus have Tl isotope compositions that are offset from

164   seawater   by   a   near-constant   fractionation   factor   of α =   1.0019

165   (α $\square\square^{205}$Tl/^{203}Tl$_{FeMn}$/^{205}Tl/^{203}Tl$_{SW}$.) This offset is thought to reflect equilibrium isotope

166   fractionation of Tl during sorption and/or subsequent oxidation of Tl(I) to Tl(III) on the

167   surfaces of Fe-Mn oxyhydroxide particles (Peacock and Moon, 2012; Rehkämper et al., 2004;

168   Rehkämper et al., 2002). However, an alternative explanation whereby the isotopic difference

169   reflects fractionation of Tl between dissolved seawater Tl$^+$ and Tl^{3+} cannot be ruled out based

170   on the currently available data (Rehkämper et al., 2004; Rehkämper et al., 2002). Regardless

171   of the exact origin, the observed extent of Tl isotope fractionation has recently been shown in

172   a theoretical study (Schauble, 2007) to be in accord with the large equilibrium isotope

173   fractionation that is expected to occur between Tl(I) and Tl(III) due to contributions from both

174   mass dependent and mass independent (nuclear volume or nuclear field shift) isotope effects.

175   Diagenetic   Fe-Mn   nodules   (which   include   primarily   samples   of   mixed

176   diagenetic/hydrogenetic origin) and hydrothermal Fe-Mn deposits from diffuse fluid flows in

177   the distal parts of hydrothermal systems display significantly more variability in Tl isotope

178   compositions, with ε^{205}Tl values that range from values of about -6 to +9 (Fig. 1). The origin

179   of this variability is currently unclear and has been ascribed to differences in fluid

180   compositions (seawater vs. diagenetic pore fluids or diffuse hydrothermal flows) or sorption

181   conditions (closed vs. open system Rayleigh fractionation, variable temperatures of

182   hydrothermal fluids) (Rehkämper et al., 2004; Rehkämper et al., 2002). Alternatively, they

183   may also be due to differences in the mineralogy of the manganese oxide phases to which Tl

184   is bound in Fe-Mn sediments (Koschinsky and Hein, 2003; Peacock and Moon, 2012). Whilst

185   the Mn mineralogy of hydrogenetic Fe-Mn crusts is almost completely dominated by

186   hexagonal birnessite, both birnessite and todorokite are present in diagenetic Fe-Mn nodules

187   and hydrothermal deposits (Burns and Burns, 1977).

188   Also of considerable interest are the Tl isotope time-series data that were recently

189   obtained for a number of Fe-Mn crusts (Nielsen et al., 2011; Nielsen et al., 2009a; Rehkämper

190   et al., 2004) and which extend back to the late Cretaceous (Fig. 2). These records are

191   relatively constant for the last 40 Myr but display a dramatic shift in ε^{205}Tl from values of

192   about +6 at 55 Myr to about +12 at 45 Myr. Both Rehkämper et al. (2004) and Nielsen et al.

193   (2009a) argue that the observed trends are (i) not due to diagenetic alteration and (ii) unrelated

194   to changes in the mineralogy or major element composition of the samples. The trends were

195   therefore interpreted as primary features that record a change in either (i) the isotope

196   fractionation factor of Tl between the Fe-Mn crusts and seawater ($\alpha_{FeMn-sw}$) or (ii) the Tl

197   isotope composition of the oceans. It is notable that the Cenozoic Tl isotope record is similar

198   in structure to both the benthic foraminiferal δ^{18}O curve (Zachos et al., 2001) and the

199   Cenozoic seawater S isotope record determined from marine barites (Paytan et al., 1998),

200   which may suggest causal links between the processes driving the respective isotopic

201   variations (Fig. 2). The δ^{18}O curve of benthic foraminifera in the Paleocene and Early Eocene

202   mainly records changes in water temperature between ~6 and 12°C (Zachos et al., 2001)

203   whereas the increase in marine S isotopes during the Early Eocene most likely reflects

204   increased pyrite burial rates (Kurtz et al., 2003) and thus a perturbation of the global carbon

205   cycle.

206   Whatever the link with Tl isotopes, it is evident that it is important to obtain an improved

207   understanding of the Tl isotope records preserved in Fe-Mn sediments, as these appear to be

208   linked to significant changes in marine conditions and the Earth's carbon cycle, which may

209   both have an important impact on global climate.

210

3. Experimental methods

3.1. Batch Tl sorption experiments

213   Three groups of batch experiments are described in this paper: (1) a time series, with

214   identical concentrations of synthetic birnessite and aqueous thallium and durations ranging

215   from 3 min to 72 hr; (2) a set of experiments at three different temperatures with varied

216   concentrations of birnessite and aqueous Tl; and (3) a set with much lower concentrations of

217   aqueous Tl than the others. For all experiments, hexagonal K-birnessite was synthesized

218   following the methods of Barling and Anbar (2004) by mixing 24 mL of 2 M HCl (distilled)

219   with 0.6 g $KMnO_4$ and allowing this mixture to react and precipitate while constantly

220   agitated. After 48 hours, the mixture was diluted to ~500 mL with 18.2 MΩ-cm water and

221   then raised to circumneutral pH by addition of NaOH pellets. This suspension was poured

222   through a polyethersulfone filter membrane with 0.45 µm pores. The birnessite was rinsed

223   with 500 mL of 18.2 MΩ-cm water four times, resuspended from the filter with more water,

224   and then suspended in 500 mL of 18.2 MΩ-cm water. A few microliters of 1 M NaOH were

225   added, and a mixture of nitrogen plus 382 ppm CO_2 was sparged through the suspension for a

226   few hours until pH stabilized at ~7. The material was kept wet at all times to avoid

227   recrystallization, and, although the crystals remain stable for long periods, a separate batch

228   was freshly made for each of the three sets of experiments in order to avoid any potential

10

229   problems from mineralogical transformation over time. An aliquot of the birnessite stock was

230   dried down, dissolved, and analyzed by ICP-MS; from this analysis we know that our

231   birnessite stock contained approximately 0.8 mg of birnessite per gram of stock suspension.

232   Previous batches of birnessite made in the same way were analyzed by X-ray diffraction (J.

233   Post, Smithsonian Institution) and determined to be poorly crystalline hexagonal K-birnessite

234   (Wasylenki et al., 2008).

235   A thallium stock solution with 49.6 μg/g Tl was prepared by dissolving reagent grade

236   TlCl in 18.2 MΩ-cm water with 0.2 M KNO_3 as background electrolyte. This solution was

237   also sparged with nitrogen + 382 ppm CO_2, and the pH was adjusted to ~7 with NaOH. A

238   second Tl stock solution was prepared at 27.0 μg/g Tl for the low Tl concentration

239   experiments.

240   The first set of experiments was performed in order to investigate how quickly Tl

241   isotopic equilibrium was reached. Here, each of six 50 mL polypropylene centrifuge tubes

242   was filled with 25 g of 49.6 μg/g Tl stock solution, 2 g of birnessite suspension, and 18 g of

243   18.2 MΩ-cm water (Table 1). Ionic strength was therefore 0.11 M in each tube and [Tl] ≈ 28

244   μg/g (Table 1). All tubes were shaken in a temperature-controlled shaker (Eppendorf

245   Thermomixer R) at 22°C. After shaking for the designated duration, each mixture was filtered

246   through a polyethersulfone membrane with 0.2 μm pores, and both fluid and solid portions

247   were collected for concentration and isotope analysis. A few drops of fluid always stuck to the

248   bottom of the filter assembly, so approximately 0.5-1 g of fluid was lost from each

249   experiment. Hence, to compute the proportion of Tl that sorbed in each experiment, we

250   divided the amount of Tl recovered in the solid portion by the total amount put in the

251   experiment (see section 5.1 for further discussion of sample recovery and mass balance). The

252   loss of fluid has no consequence for the isotope systematics, since all fluids and solids were

253   measured directly for Tl isotope composition.

254   The second set of experiments was designed to investigate how Tl isotope

255   fractionation varies as function of temperature and fraction of Tl sorbed. A range of

256   temperatures that encompasses most of those encountered in the marine environment was

257   chosen. At each temperature (6°, 25°, 40°C), the proportions of Tl and birnessite were varied.

258   In each experiment, an aliquot of 49.6 μg/g Tl stock solution (3 to 10 mL) was mixed with an

259   aliquot of birnessite stock (250 to 2000 μL) plus 18.2 MΩ-cm water in a polypropylene

260   centrifuge tube. These mixtures resulted in [Tl] ≈ 25 μg/g (Table 1). Ionic strength was 0.10

261   M in each experiment, and pH was again ~7. The mixtures were shaken at either 6°, 25°, or

262   40°C. Experiments conducted at 6° C and 25° C ran for 50 and 48 hours, respectively,

263   whereas the 40°C experiments were terminated after just two hours to avoid recrystallization

264   of birnessite to other Mn oxide minerals during the experiment. Experiments that were

265   conducted at 50°C are not included in this paper, as they showed clear signs of change in

266   grain size and aggregation behaviour after 48 hr, presumably because recrystallization of

267   birnessite to another manganese phase had begun.

268   A small, weighed aliquot of each recovered fluid was used for the measurement of Tl

269   concentrations by ICP-MS. Recovered birnessite particles with sorbed Tl were dissolved with

270   warm ~3 M HCl, and a small aliquot of each sample was used for Tl abundance

271   determination. The amounts of Tl in the portions of each experiment and the percentages of Tl

272   sorbed are listed in Table 2. Rigorous propagation of uncertainties is difficult, since the

273   greatest source of error is likely the sample handling, rather than the analytical measurements.

274   Error bars in plots have been propagated from an estimated 5% relative uncertainty on each Tl

275   amount (Prytulak et al., 2013). Further aliquots of each fluid and digested birnessite sample

276   were taken for isotopic analyses, which were performed according to methods described

277   below.

278   The third set of experiments was performed with much lower initial Tl concentrations as

279   it was suspected that the amounts of Tl added to the experiments were partially controlling the

280   observed isotope fractionation factors. Here, about 0.25 g of a 27.0 μg/g Tl stock solution and

281   ~0.5 g of birnessite stock (corresponding to about 0.4 mg of birnessite) were mixed with

282   variable amounts (~15 to 45 g) of a 0.1 M KNO_3 solution (Table 3). These mixtures resulted

283   in starting Tl concentrations between ~0.1 and 0.4 μg/g, two orders lower than in the previous

284   experiments, which ranged from 25 to 28 μg/g Tl. Temperature was 22°C, ionic strength was

285   0.1 M, *p*H was ~7, and experimental duration was 44 hours. Samples were prepared for Tl

286   isotope analysis using similar methods to those applied in the other experiments.

287

288   **3.2. Thallium separation and isotope composition analysis**

289   Before chemical separation of Tl, all samples were evaporated to dryness and re-

290   dissolved in 1 M HCl. Subsequently, 18 MΩ-cm water saturated with ~1% (vol/vol) Br_2 was

291   added in order to oxidize Tl to the trivalent state required for the column chemistry procedure

292   (Rehkämper and Halliday, 1999). Chemical separation of Tl from the sample matrix (mainly

293   Mn and K) was performed with the anion exchange resin AG1-X8 in 100 μL resin bed

294   columns using previously described techniques (Nielsen et al., 2004; Nielsen et al., 2005;

295   Rehkämper and Halliday, 1999).

296   Isotope compositions for time and temperature series were measured on Nu Plasma MC-

297   ICPMS instruments in the MAGIC labs at Imperial College London and Oxford University,

298   respectively, while low-Tl experiments were measured on a Thermo Finnigan Neptune MC-

299   ICPMS at Woods Hole. These analyses applied previously established techniques, whereby

300   the $^{208}Pb/^{206}Pb$ isotope ratio of an admixed solution of NIST SRM 981 Pb is used to correct

301   for the instrumental mass bias of the measured $^{205}Tl/^{203}Tl$ ratio, using the exponential law in

302   combination with standard sample bracketing (Baker et al., 2009; Nielsen et al., 2004;

303   Rehkämper et al., 2002). The corrected ^{205}Tl/^{203}Tl ratios of the samples are reported here

304   relative to the NIST SRM 997 Tl standard following equation (1)

305   Based on replicate measurements of standard solutions and some of the samples, all

306   analyses are assigned an uncertainty of ±0.3 ε^{205}Tl. The precision of the results was

307   furthermore ascertained by repeated analyses of the secondary Aldrich Tl reference material

308   (Nielsen and Rehkämper, 2011; Rehkämper et al., 2002) and solutions of NIST SRM 997 Tl

309   that were processed through the column chemistry. All these tests were consistent with the

310   assigned error of ±0.3 ε^{205}Tl. With the most recent generation of MC-ICPMS instruments,

311   precise and accurate Tl isotope data can be generated even for <1ng of Tl (Nielsen et al.,

312   2007; Nielsen et al., 2006b; Nielsen et al., 2009b) and given that all experimental run products

313   contained >2ng of Tl, none of the analyses were compromised by low Tl ion beam intensities.

314   The fractionation factors between two samples A and B are expressed in terms of α, where

315        $$\alpha_{A\text{-}B} = (^{205}\text{Tl}/^{203}\text{Tl}_A)/(^{205}\text{Tl}/^{203}\text{Tl}_B) \approx (\varepsilon^{205}\text{Tl}_A + 10000)/(\varepsilon^{205}\text{Tl}_B + 10000). \qquad (2)$$

316   The uncertainty on α is the square root of the sum of the uncertainties squared of the two

317   isotopic measurements, which is about ±0.00004.

318

319   **4. Results**

320   Results from our experiments are tabulated in Tables 1, 2, and 3 and shown graphically

321   in Figs. 3-6. In all experiments, the isotopic composition of sorbed Tl is heavier than that of

322   aqueous Tl remaining in the fluid. The six time series experiments had nearly identical

323   concentrations of birnessite and Tl (see Table 1), and the resulting proportions of Tl sorbed

324   and dissolved are nearly the same regardless of experimental duration (Table 2). Isotopic

325   fractionation   between   sorbed   and   dissolved   Tl   in   these   experiments

326   ($\alpha = {}^{205}\text{Tl}/^{203}\text{Tl}_{sorbed}/^{205}\text{Tl}/^{203}\text{Tl}_{dissolved}$) is almost constant within analytical uncertainties,

327   although the values show a very slight increase over time from 1.00021 at 3 min to 1.00031

328 after 72 hr (Fig. 3). We note that these fractionations are much smaller than those observed

329 between seawater and natural ferromanganese sediments, and possible reasons for this

330 discrepancy are discussed below.

331   The temperature dependent experiments all had nearly the same initial aqueous [Tl], but

332 varied amounts of birnessite. This led to a wide range in the fraction of sorbed Tl (Fig. 4a)

333 and in the amount of Tl sorbed per milligram of birnessite (Fig. 4b). The isotope fractionation

334 factors in these experiments ranged from $\alpha_{sorbed-dissolved} \approx 1.0004$ to 1.0007 and are highly

335 correlated with the fraction of Tl sorbed and the amount of Tl sorbed per milligram birnessite.

336 The largest fractionations were recorded for the highest fractions of sorbed Tl, and since these

337 experiments contained more birnessite, the concentrations of Tl in the final solids were lower.

338   Experiments performed with low initial Tl concentrations (≤ 0.4 μg/g, rather than ~25

339 μg/g) exhibit the largest isotope fractionation factors between $\alpha \approx 1.00098$ and 1.00145

340 (Table 3) and are thus closest to agreeing with the fractionation observed between seawater

341 and natural hydrogenetic Fe-Mn crusts ($\alpha \approx 1.0019$ to 1.0022; Rehkämper et al., 2002). The

342 four experiments were performed with nearly identical amounts of birnessite and Tl, but the

343 volume of 0.1 M KNO_3 used to dilute the Tl stock solution varied (Table 1), which means that

344 the starting Tl concentration was the only physical parameter that varied in this set of

345 experiments. The Tl isotope fractionation factor correlates inversely with starting aqueous

346 [Tl], i.e. linearly with 1/[Tl] (Fig. 6), with the largest fractionation observed for the

347 experiment with the lowest initial aqueous [Tl].

348

349 **5. Discussion**

350 **5.1. Assessment of Tl recovery from experiments**

351   Using the measured isotopic compositions and concentrations of our Tl stock solutions

352 (Table 1), we have compared the total amount of Tl put into each experiment to the sum of the

353   amount recovered in the fluid and the solid portions, in order to assess how well Tl was

354   recovered. Note that because we measured the isotopic composition of Tl in every fluid and

355   solid, some loss of Tl from either pool is of no consequence for determining the isotopic

356   fractionation expressed in each experiment, as long as the reasonable assumption is made that

357   the fractions of fluid and solid lost were isotopically identical to those recovered. However,

358   failure to recover all of the Tl in the experiment does introduce some error into our

359   determination of the fraction of Tl sorbed or the amount of Tl sorbed per mg of birnessite, and

360   the error in this case is difficult to quantify rigorously. Therefore, we employ an isotopic mass

361   balance calculation to determine the fraction sorbed in each experiment.

362    $$\varepsilon^{205}Tl_{stock} = \varepsilon^{205}Tl_{dissolved} * f_{dissolved} + \varepsilon^{205}Tl_{sorbed} * f_{sorbed} \qquad (3)$$

363   Here, $\varepsilon^{205}Tl_{stock}$, $\varepsilon^{205}Tl_{dissolved}$ and $\varepsilon^{205}Tl_{sorbed}$ are the isotope compositions of the stock

364   solution, fluid phase and solid phase Tl, respectively, whilst $f_{dissolved}$ and f_{sorbed} denote the mass

365   fractions of Tl in the fluid and solid phases and these values add up to 1. Since we know the

366   isotopic compositions of all three components in equation 3 we can determine the fraction

367   sorbed by substituting $f_{dissolved}$ for 1- f_{sorbed}. The amount of Tl sorbed per mg of birnessite

368   reported in Table 3 is calculated with this method and we use these values throughout all

369   figures.

370

371   **5.2. Thallium sorption sites**

372   Thallium sorbed to hexagonal birnessite has previously been shown to be oxidized to

373   Tl(III), with Tl sorbed as an inner-sphere complex over Mn vacancies in the phyllomanganate

374   sheets, and this difference in Tl oxidation state between solution and solid could well drive

375   isotopic fractionation (Peacock and Moon, 2012). In similar sorption experiments to those

376   here, it has been shown that Ni also sorbs to birnessite as an inner-sphere complex over Mn

377   vacancies (Manceau et al., 2007; Peacock and Sherman, 2007) and it has been estimated that

16

378 crystalline birnessite can accommodate ~1.4 wt% Ni via this sorption mechanism (Peacock,

379 2009). This corresponds to 0.24 mmol Ni/g birnessite. If the molar capacity for Tl at this site

380 were the same, then the maximum concentration of Tl in Tl-sorbed birnessite would be

381 approximately 5 wt% (or ~53 μg Tl sorbed per g birnessite). Our experiments were performed

382 using poorly crystalline birnessite, which has a larger surface area and therefore might have a

383 higher sorption capacity than that estimated based on the Ni experiments described above.

384 Additional uncertainty should also be considered given that Tl and Ni also sorb via somewhat

385 different processes (only Tl is oxidized during the sorption process). However, we estimate

386 that vacancy sites are unlikely to accommodate more than 5-15 wt% Tl. All of our

387 experimental products have more than 14 wt% Tl associated with the solid (up to 32 wt%),

388 which leads us to hypothesize that some Tl in our experiments is sorbed over vacancy sites,

389 but additional Tl is sorbed in a different manner. The overall isotope fractionation we observe

390 in our experiments would then be a combination of strongly fractionated, inner-sphere-over-

391 vacancy Tl and another pool of Tl with unknown oxidation state that is unfractionated or only

392 slightly fractionated from solution (hereafter designated as 'slightly fractionated').

393   If the amount of sorbed Tl in our experiments exceeds the sorption capacity of sites over

394 Mn vacancies, what could the other sorbed species be? A comprehensive answer to that

395 question is beyond the scope of this study, but Tl(I) may be able to sorb loosely, as an outer-

396 sphere complex, and/or strongly, as an inner-sphere complex onto MnOH sites located at the

397 edges of the phyllomanganate sheets (hereafter referred to as 'edge sites'). Neither of these

398 sorption mechanisms is expected to result in oxidation of Tl(I) to Tl(III) (Peacock and Moon,

399 2012), and thus little or no fractionation of isotopes is expected to occur between this pool of

400 sorbed Tl and Tl remaining dissolved in solution. The latter mechanism of inner-sphere

401 sorption to edge sites has been observed previously for Ni on vernadite at high Ni surface

402 loading, when the vacancy sites are saturated (Manceau et al., 2007).

403   Even though Tl and Ni both sorb to birnessite as inner-sphere complexes at Mn vacancy

404   sites, only Tl sorption involves oxidation of the sorbing species and coupled reductive

405   dissolution of the birnessite phase (Peacock and Moon, 2012). This difference in oxidation

406   between Tl and Ni is important because it has been shown that oxidation of redox-active

407   metals at hexagonal birnessite surfaces (our starting material) can induce a rapid structural

408   ripening and conversion to triclinic birnessite and potentially todorokite (Bargar et al., 2005;

409   Learman et al., 2011; Webb et al., 2005), which leads to a dramatic decline in the oxidative

410   capacity of the Mn oxide (Learman et al., 2011). Triclinic birnessite and todorokite still have

411   the potential to sorb significant amounts of Tl, but do not cause any Tl oxidation (Peacock and

412   Moon, 2012) and hence are unlikely to be associated with Tl isotope fractionation. Thus our

413   slightly fractionated Tl could be at least partially located at sorption sites of triclinic birnessite

414   or todorokite that continuously form while the hexagonal birnesiste vacancy sites become

415   occupied.

416   We also considered the possibility that birnessite may continue to oxidize additional Tl(I)

417   to Tl(III), even if all above-vacancy sites are saturated, and that the excess oxidized Tl could

418   precipitate as Tl_2O_3. However, experimental evidence to date shows that phyllomanganates

419   (triclinic birnessite) and tectomanagnates (todorokite), both devoid of vacancy sites, are

420   unable to oxidise Tl, and thus oxidative sorption of Tl is associated with vacancy site sorption

421   only (Peacock and Moon, 2012). We also conducted a scaled-up version of one of our 25 °C

422   experiments (Tl-25-01, with 63% of Tl sorbed and a final solid with 17 wt% Tl) to produce

423   enough solid for X-ray diffraction analysis, but the resulting diffraction pattern (not shown)

424   had only broad peaks consistent with poorly crystalline birnessite, with none of the peaks

425   expected for Tl_2O_3.

426   Based on the above discussion, we conclude that Tl in our experiments is sorbed to at

427   least two different sites, one of which is as an inner-sphere complex over vacancies in

428   hexagonal birnessite. The remaining Tl could either be sorbed as outer-sphere complexes, as

429   inner-sphere complexes to edge sites and/or associated with triclinic birnessite or todorokite

430   that continuously form due to electron transfer processes occurring as part of the Tl oxidative

431   sorption at vacancy sites.

432

433   **5.3. Time and temperature dependent experiments**

434   The first-order observation for all experiments is a heavier isotopic composition of Tl

435   sorbed onto birnessite relative to that left in solution. This sense of fractionation is consistent

436   with Tl isotope data for natural marine ferromanganese crusts (Fig. 1), which all exhibit heavy

437   isotope compositions compared to the seawater from which they precipitated (Rehkämper et

438   al., 2004; Rehkämper et al., 2002). Because the sorbed Tl is heavier, we infer right away that

439   the fractionation cannot be simply a kinetic effect, whereby lighter Tl sorbs more rapidly.

440   Rather, the fractionation we see in experiments and nature involves at least one equilibrium

441   step, possibly a Rayleigh process, or a combination of kinetic and equilibrium effects.

442   In our time series experiments (Fig. 3), the data indicate a slight increase in the

443   magnitude of fractionation over the first 24 hours. This suggests that a small kinetic isotope

444   effect may overprint an equilibrium fractionation in our shortest duration experiments, but

445   such a small, short-lived effect is very unlikely to have any importance in fractionations

446   recorded in marine ferromanganese sediments and is not discussed further.

447   The fractionation factors we observe in the time series experiments ($\alpha_{sorbed-dissolved}$ =

448   1.00021 to 1.00031) are all much lower than those observed between natural samples and

449   seawater (Fig. 1), where $\alpha_{FeMn-seawater} \approx 1.0020$ for hydrogenetic Fe-Mn crusts and $\alpha_{FeMn-seawater}$

450   ≈ 1.0006 to 1.0015 for diagenetic Fe-Mn deposits (Rehkämper et al., 2004; Rehkämper et al.,

451   2002). Our time series fractionation factors are also smaller than theoretical predictions of

19

452 equilibrium fractionation between Tl(I) and Tl(III) *in vacuo* ($\alpha \approx$ 1.0025-1.0027 at 22° C)

453 (Schauble, 2007).

454 The most likely explanation for the discrepancy between our experimental results and

455 those from nature and theory is that the solids in our experiments contain several orders of

456 magnitude more Tl than in nature (1 – 30 wt% vs. 0.001-0.01 wt% (Hein et al., 2000;

457 Rehkämper et al., 2002)) and hence other sorption sites appear to be utilized (see section 5.2.)

458 Other potential explanations could be that the experiments were conducted at different

459 pH and ionic strength than the conditions of Fe-Mn crust precipitation. Since pH strongly

460 affects the sorption capacity of solids, it is also possible that isotope fractionation is affected

461 by variable pH. We did not vary the pH of our experiments (all were conducted at pH ~7) and

462 it is therefore not possible with our present data set to evaluate if pH has a strong effect on Tl

463 isotope fractionation during sorption to birnessite. Our experiments contain 0.1 M KNO_3, but

464 seawater contains ~0.5 M NaCl. Thallium is therefore initially present as Tl^+ in our

465 experiments, but may exist as a combination of Tl^+, $TlOH^0_{(aq)}$ and $TlCl^0_{(aq)}$ in seawater

466 (Byrne, 2002; Nielsen et al., 2009a). Whether the difference in coordination chemistry for Tl

467 as a function of ionic strength and [Cl^-] could influence fractionation during sorption of Tl (or

468 any other metal) to such a large extent is so far unknown and should be a focus of future

469 studies.

470 There are two conclusions to draw from the second series of experiments, conducted at

471 three different temperatures, with the same initial aqueous [Tl], but varying amounts of

472 birnessite (Table 1). A clear correlation between fraction of Tl sorbed and isotope

473 fractionation factor is evident in Table 2 and Fig. 4a, but, importantly, temperature seems to

474 have little effect on isotope behaviour. At any given fraction of Tl sorbed, the difference in

475 isotope fractionation between 6° and 40° C is less than 0.0002 in terms of $\alpha_{sorbed-dissolved}$, with

476 a slight suggestion that a higher magnitude of fractionation occurs at lower temperature, as

477 expected. The magnitude of change in isotope fractionation as a function of temperature is

478 similar to predictions by Schauble (2007), who calculated that $\alpha_{Tl(III)-(I)}$ should change by

479 ~0.0003 between 6° and 40° C.

480   Another observation from Fig. 4a is that the overall fractionation expressed in our

481 experiments is correlated with the fraction of Tl in the experiment that is sorbed to birnessite.

482 This trend could be interpreted to reflect a Rayleigh distillation process, whereby Tl is

483 irreversibly sorbed to birnessite and the fluid continues to evolve to lighter compositions as

484 sorption proceeds. But this conclusion is inconsistent with the much lower fractionation

485 factors recorded for the time dependent experiments at the same fraction of Tl sorbed (Fig.

486 4a). Fig. 4b shows the same experiments with a different choice of independent variable (the

487 number of μg of Tl sorbed per mg of birnessite), and the result is a single trend for the time

488 series and temperature experiments. We did not measure the surface area of birnessite in our

489 experiments, but the mass of birnessite serves as a close proxy. The relationship shown in Fig.

490 4b supports our hypothesis that the fractionations expressed in our experiments reflect

491 different proportions of Tl sorbing in at least two different sites. One of the sites is limited in

492 number, strongly fractionated, and likely represents Tl(III) sorbed over Mn vacancies on

493 {001} surfaces (space group P6$_3$/mmc). In contrast, the other sites hold Tl that is only slightly

494 fractionated from dissolved Tl and may comprise Tl sorbed to birnessite edges or triclinic

495 birnessite formed via oxidative ripening (Learman et al., 2011).

496

497 **5.4. Low Tl experiments and sorption site mixing models**

498   To further investigate the relationship between Tl isotope fractionation and the amount of

499 Tl sorbed per unit of birnessite, we conducted the third set of experiments, each with the same

500 amount of birnessite and Tl. These experiments featured varying volumes of fluid (details in

501 Table 1) and initial concentrations of aqueous [Tl] about two orders of magnitude smaller

502 than in the earlier experiments. Results are shown in Table 3 and plotted in Figs. 5 and 6. The

503 concentrations of Tl in the solids (~17 μg Tl per mg birnessite) were the lowest of all the

504 experiments and we observed the highest fractionation factors yet ($\alpha_{\text{sorbed-dissolved}}$ = 1.0010 to

505 1.0014), although these values are still smaller than those observed in nature.

506   Figure 5 shows the low-Tl data along with results from the other experiments and the

507 data for natural hydrogenetic ferromanganese crusts from Rehkämper et al. (2002). The shape

508 of the trend formed by all of the data indeed suggests a mixing line between two pools of Tl

509 with different isotopic compositions. We calculated model mixing lines for $\alpha_{\text{sorbed-dissolved}}$ as a

510 function of μg Tl/mg birnessite (*x*), with three free parameters: the sorption capacity of

511 vacancy sites (*sorb-cap*), the fractionation factor associated with vacancy sites (*vac-frac*), and

512 the fractionation factor between dissolved Tl and our hypothesized edge sorption site (*edge-*

513 *frac*). For values of μg Tl/mg birnessite smaller than *sorb-cap*, $\alpha_{\text{sorbed-dissolved}}$ is simply equal to

514 *vac-frac* because it is assumed that the vacancy sites fill up before any of the edge sites are

515 utilized. For values of μg Tl/mg birnessite greater than *sorb-cap*, $\alpha_{\text{sorbed-dissolved}}$ is computed as

516 a linear combination of fractionated and slightly fractionated Tl, with all vacancy sites filled

517 up to *sorb-cap* and the remainder of sorbed Tl on edge sites:

518                   $\alpha_{\text{sorbed-dissolved}}$ = ((*sorb-cap**vac-frac + (*x* - *sorb-cap*)*(*edge-frac*)) / *x*.   (4)

519 We present two of our best-fit model curves. Model 1 has a low value for *sorb-cap* of 5 μg

520 Tl/mg birnessite, *vac-frac* = 1.0020, and *edge-frac* = 1.0003. The curve misses some of the

521 temperature dependent data, but fits the rest quite well. Model 2 has a higher sorption capacity

522 of 28 μg Tl/mg birnessite, *vac-frac* = 1.0023, and *edge-frac* = 1.0002. This curve fits our

523 high-Tl experiments better, but overestimates the fractionation factors for low-Tl experiments

524 and natural data. This simple model is built on the presumption that the above-vacancy sites

525 are high affinity sites and thus fill first, and all remaining Tl that sorbs does so via edge sites.

526 That we cannot find values for the three parameters that result in a good fit to all data suggests

527 that this presumption is incorrect. Perhaps Tl partitioning onto the two types of sorption sites

528 is simultaneous but the vacancy sites have higher affinity for Tl and thus fill up first. The

529 number of vacancy vs. edge sites, and thus the rate at which the two sorption sites fill, would

530 then depend on the crystallinity of the birnessite, and/or could vary with the amount of sorbed

531 Tl or as a function of aqueous [Tl] (Fig. 6). Such mechanisms are not inconsistent with our

532 high-Tl experiments as, presumably, all vacancy sites are filled and thus these experiments do

533 not inform on the rate at which the two types of sorption sites fill.

534

535 **5.5. An alternative to sorption site mixing**

536 Figure 6 shows an interesting correlation between the starting concentration of Tl in the

537 low-Tl experiments and the isotope fractionation factor that may shed a bit more light on the

538 factors controlling the observed correlation. These experiments contained essentially the same

539 amount of Tl (6.7 μg) and the same amount of birnessite (0.4 mg), but had different initial

540 aqueous Tl concentrations, since the total volume of the experiments varied. There is a strong

541 linear correlation between the inverse of the initial aqueous [Tl] and fractionation factor (Fig.

542 6). First, we note that the relationship illustrated here serves as more evidence that our data do

543 not reflect a simple equilibrium isotope effect, because the concentration of the solution

544 would not affect the isotope fractionation factor, if a simple equilibrium between just two

545 pools (dissolved and sorbed Tl) was attained. Next, we can use the insight from the EXAFS

546 work of Peacock and Moon (2012) to speculate about an alternative mechanism, other than

547 partitioning of Tl into different sorption sites, that could lead to larger fractionation factors at

548 lower aqueous Tl concentrations.

549 We know that birnessite causes surface oxidation of aqueous Tl^+ to Tl^{3+}, which is

550 adsorbed onto the birnessite structure (Peacock and Moon, 2012). In principle, we can

551 therefore construct a simplified isotope exchange reaction that may be predominantly

552 responsible for the Tl isotope fractionation in birnessite:

553
$$Tl^+_{(aq)} \rightleftarrows Tl^{3+}_{(s)} + 2e^- \qquad (5)$$
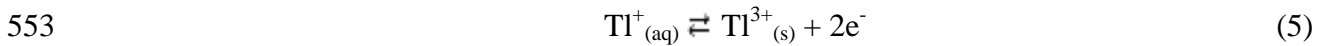
554 In this reaction, an increase in the concentration of Tl in solution will tend to push the

555 equilibrium reaction towards the right, thereby increasing the rate of the forward reaction

556 relative to the reverse process. In this way, higher Tl concentrations in solution could result in

557 longer equilibration times. However, there is no indication in our time series data that the

558 isotope fractionation factor continues to increase for more than ~20 hr (Fig. 3), which would

559 imply that the low-Tl experiments had sufficient time to reach their maximum isotope

560 fractionation as these were conducted at much lower Tl concentrations than the time series

561 (Table 1). Therefore, we cannot explain the variable α in the low-Tl experiments solely by

562 considering reaction (5).

563 We can, however, break down the Tl isotope fractionation process into separate reactions

564 that are together responsible for Tl sorption, oxidation and isotope fractionation. Peacock and

565 Moon (2012) have proposed that Tl oxidation likely takes place while Tl^+ is loosely bound

566 (LB) to birnessite as an outer-sphere complex. Thus we can write the following two reactions

567 to account for the Tl isotope fractionation:

568
$$Tl^+_{(aq)} \rightleftarrows Tl^+_{(LB)} \qquad (6)$$

569
$$Tl^+_{(LB)} \rightleftarrows Tl^{3+}_{(LB)} + 2e^- \qquad (7)$$
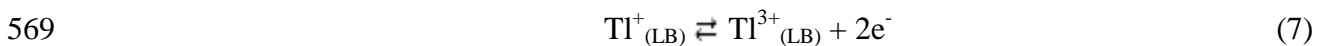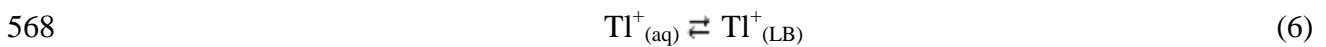
570 The oxidation reaction (7) will be followed by adsorption of the oxidized Tl onto the

571 birnessite structure. On the time scale of the experiments, the latter process is probably

572 essentially unidirectional because the trivalent Tl is very strongly bound to the birnessite

573 surface (Peacock and Moon, 2012):

24

$$Tl^{3+}_{(LB)} \rightarrow Tl^{3+}_{(s)} \qquad\qquad (8)$$

574
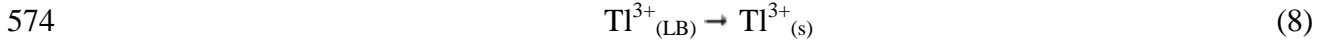
575   Each of these three reactions (6, 7 and 8) account for a separate part of the total reaction

576 (5) whereby aqueous, monovalent Tl is first attracted to a sorption site and loosely bound as

577 an outer-sphere complex with no isotope fractionation (6), then it is oxidized and isotopically

578 fractionated while still loosely bound (7) and lastly adsorbed as an inner-sphere surface

579 complex at the vacancy sites with no isotope fractionation (8). During our experiments we

580 measured the isotopic difference between $Tl^+_{(aq)}$ and $Tl^{3+}_{(s)}$, which means we were not directly

581 measuring the isotope fractionation factor in (7), but the sum of the three reactions (6, 7 and

582 8). This limitation is important because the reaction kinetics of all three reactions will

583 determine how much of the isotope fractionation generated in (7) will be expressed in our

584 measurements. For example, we can consider a situation in (7) at isotopic equilibrium where

585 one half of the Tl is trivalent and the other half monovalent. If $\alpha = 1.002$ then we can

586 determine that $\varepsilon^{205}Tl^{3+} = +10$ and $\varepsilon^{205}Tl^+ = -10$, compared with the starting solution. Any

587 $Tl^{3+}_{(LB)}$ sorbed onto birnessite at this point would have an apparent $\alpha = 1.001$. But at the same

588 time, reaction (6) will drive $\varepsilon^{205}Tl^+$ back toward the isotope composition of the starting

589 solution and thus the relative rates of oxidation (7) and isotope re-equilibration (6) will

590 determine the isotope composition of the $Tl^{3+}_{(LB)}$, which is what we measure on the birnessite.

591   Using these reaction principles we can understand why the Tl concentration of the

592 starting solution may have such a profound impact on the observed α, because

593 thermodynamics dictate that increased concentrations on the left hand side of a reaction will

594 enhance the rate of the forward reaction relative to the back reaction. The impact of the back

595 reaction in (6) is thereby controlled by the Tl concentration of the solution, which translates

596 directly to isotope fractionation if isotope equilibration is slower in (6) than in (7). If we

597 furthermore assume that reaction (8) is essentially unidirectional at the timescale of our

598 experiments, it can be shown by simple modelling, that the relationship seen in Fig. 6 may

599   result from a dampening of the expressed isotope fractionation, which is enhanced at higher

600   initial dissolved Tl concentrations.

601   Hence, we have two possible explanations for the correlation between isotope

602   fractionation factor and initial solution concentration observed for the low-Tl experiments:

603   namely, a mixing relationship produced by the simultaneous occupation of both vacancy and

604   edge sites by Tl during sorption, or the latter kinetic model. However, given the complexities

605   of the kinetic model, it is debatable whether this can reasonably account for the systematics

606   seen in Fig. 6. Therefore, we currently favour the explanation in which the Tl isotope

607   composition of all our experiments (low- and high-Tl) can be explained by simultaneous

608   occupation of both vacancy and edge sites by Tl during sorption. This mechanism may

609   potentially also operate in nature, which could cause variations in the effective Tl isotope

610   fractionation during sorption to Fe-Mn oxyhydroxides. However, the correlation in Fig. 6

611   would imply that the full isotope fractionation factor (and hence that only vacancy sites are

612   utilized) should occur at solution concentrations below 0.080 μg/g, which is more than three

613   orders of magnitude more concentrated than seawater. Thus, based on our data we would

614   predict essentially no variation in isotope fractionation during sorption of Tl from seawater

615   onto birnessite, which is consistent with the almost constant fractionation factor observed in

616   nature between hydrogenetic Fe-Mn crusts and seawater (Rehkämper et al., 2002). On the

617   other hand, given the mineralogical heterogeneity of manganese oxides in diagenetic and

618   hydrothermal Fe-Mn deposits (Burns and Burns, 1977), it is equally expected that Tl isotope

619   fractionation is highly variable in these types of Fe-Mn sediments (Peacock and Moon, 2012).

620

6. Conclusions and outlook

622   We have conducted the first study of Tl isotope fractionation during sorption of aqueous

623   Tl(I) onto the manganese oxide birnessite. Experiments conducted at high Tl solution

624 concentrations (~25-28 μg/g) display relatively small isotope fractionation factors of $\alpha \approx$

625 1.0002 to 1.0007 and Tl concentrations up to 34 wt% (430 μg Tl/mg birnessite). We conclude

626 that both fractionated (adsorbed at vacancy sites) and slightly fractionated (sorbed at edge

627 sites or oxidatively formed triclinic birnessite) Tl is associated with the birnessite in these

628 experiments, and the overall fractionation expressed in each experiment reflects the difference

629 between the isotopic compositions of Tl in solution and a weighted combination of the two

630 pools of sorbed Tl.

631 We observe changes of less than 0.0002 in $\alpha_{sorbed-dissolved}$ when changing the temperature

632 from 6° to 40°C, which is consistent with predictions made from theoretical calculations of Tl

633 isotope fractionation (Schauble, 2007). As such, the temperature dependence of Tl isotope

634 fractionation in Fe-Mn crusts is likely to be negligible as deep ocean water temperatures in the

635 Cenozoic have not varied by more than 10°C (Zachos et al., 2001).

636 Experiments performed at lower Tl solution concentrations (about 0.15 to 0.46 μg/g)

637 display higher fractionation factors ($\alpha \approx$ 1.0010-1.0015), which correlate with the reciprocal

638 of initial dissolved Tl concentrations. We cannot presently determine a unique mechanism to

639 explain this correlation. Most likely, the correlation is caused by simultaneous filling of

640 vacancy sites and an unknown sorption site, whereby more monovalent Tl is partitioned to the

641 slightly fractionated with increasing solution concentration. Alternatively, a Rayleigh type

642 distillation process in which the isotope fractionation factor is dampened at increasing

643 solution concentrations may also explain the observed correlation.

644 Our results are consistent with the recently proposed oxidation-adsorption reaction for

645 sorption of Tl onto birnessite (Peacock and Moon, 2012). By combining isotopic and

646 mineralogical considerations we suggest that Tl isotope fractionation for birnessite vacancy

647 sites occurs in three steps: first, aqueous Tl is sorbed as a loosely bound univalent outer-

648 sphere complex, which is then oxidized to Tl(III) and finally adsorbed onto the birnessite

649   structure. Thallium isotope fractionation only occurs during the oxidation reaction, whereby

650   nuclear field shift effects may produce fractionation factors of several permil (Schauble,

651   2007). However, more work is required in order to obtain a full understanding of the

652   mechanisms that produce the large Tl isotope fractionation in nature between Fe-Mn crusts

653   and seawater. In particular, it will be important to ascertain if our hypothesis that two types of

654   sorption sites were occupied in our experiments is correct. In addition, further experiments are

655   needed to investigate the proposed mineralogical control of Tl isotope fractionation during

656   sorption to Fe-Mn deposits (Peacock and Moon, 2012) as well as to assess whether

657   parameters such as pH and ionic strength could affect the Tl isotope fractionation factors.

658

666

8. References

Baker, R.G.A., Rehkämper, M., Hinkley, T.K., Nielsen, S.G., Toutain, J.P., 2009. Investigation of thallium fluxes from subaerial volcanism-Implications for the present and past mass balance of thallium in the oceans. Geochim. Cosmochim. Acta. 73, 6340-6359.

Bargar, J.R., Tebo, B.M., Bergmann, U., Webb, S.M., Glatzel, P., Chiu, V.Q., Villalobos, M., 2005. Biotic and abiotic products of Mn(II) oxidation by spores of the marine Bacillus sp. strain SG-1. American Mineralogist 90, 143-154.

Barling, J., Anbar, A.D., 2004. Molybdenum isotope fractionation during adsorption by manganese oxides. Earth Planet. Sci. Lett. 217, 315-329.

Barling, J., Arnold, G.L., Anbar, A.D., 2001. Natural mass-dependent variations in the isotopic composition of molybdenum. Earth Planet. Sci. Lett. 193, 447-457.

Bidoglio, G., Gibson, P.N., Ogorman, M., Roberts, K.J., 1993. X-Ray-Absorption Spectroscopy Investigation of Surface Redox Transformations of Thallium and Chromium on Colloidal Mineral Oxides. Geochim. Cosmochim. Acta. 57, 2389-2394.

Bruland, K.W., 1983. Trace elements in seawater, in: Riley, J.P., Chester, R. (Eds.), Chemical Oceanography. Acad. Press, London, pp. 157-221.

Burns, R.G., Burns, V.M., 1977. Mineralogy of ferromanganese nodules, in: Glasby, G.P. (Ed.), Marine Manganese Deposits. Elsevier, Amsterdam.

Byrne, R.H., 2002. Inorganic speciation of dissolved elements in seawater: the influence of pH on concentration ratios. Geochemical Transactions 3, 11-16.

Flegal, A.R., Patterson, C.C., 1985. Thallium concentrations in seawater. Mar. Chem. 15, 327-331.

Flegal, A.R., Settle, D.M., Patterson, C.C., 1986. Thallium in marine plankton. Marine Biology 90, 501-503.

Frank, M., 2002. Radiogenic isotopes: Tracers of past ocean circulation and erosional input. Rev. Geophys. 40, art. no.-1001.

Gauthier, P.J., Le Cloarec, M.F., 1998. Variability of alkali and heavy metal fluxes released by Mt. Etna volcano, Sicily, between 1991 and 1995. J. Volcanol. Geotherm. Res. 81, 311-326.

Hein, J.R., Koschinsky, A., Bau, M., Manheim, F.T., Kang, J.-K., Roberts, L., 2000. Cobalt-rich ferromanganese crusts in the Pacific, in: Cronan, D.S. (Ed.), Handbook of Marine Mineral Deposits. CRC Press, Boca Raton, pp. 239-280.

Heinrichs, H., Schulz-Dobrick, B., Wedepohl, K.H., 1980. Terrestrial Geochemistry of Cd, Bi, Tl, Pb, Zn and Rb. Geochim. Cosmochim. Acta. 44, 1519-1533.

Hinkley, T.K., Lecloarec, M.F., Lambert, G., 1994. Fractionation of Families of Major, Minor and Trace-Metals Across the Melt Vapor Interface in Volcanic Exhalations. Geochim. Cosmochim. Acta. 58, 3255-3263.

Horner, T.J., Schonbachler, M., Rehkämper, M., Nielsen, S.G., Williams, H., Halliday, A.N., Xue, Z., Hein, J.R., 2010. Ferromanganese crusts as archives of deep water Cd isotope compositions. Geochem. Geophys. Geosyst. 11, doi: 10.1029/2009gc002987.

Koschinsky, A., Hein, J.R., 2003. Acquisition of elements from seawater by ferromanganese crusts: Solid phase association and seawater speciation. Mar. Geol. 198, 331-351.

Kurtz, A.C., Kump, L.R., Arthur, M.A., Zachos, J.C., Paytan, A., 2003. Early Cenozoic decoupling of the global carbon and sulfur cycles. Paleoceanography 18.

Learman, D.R., Wankel, S.D., Webb, S.M., Martinez, N., Madden, A.S., Hansel, C.M., 2011. Coupled biotic-abiotic Mn(II) oxidation pathway mediates the formation and structural evolution of biogenic Mn oxides. Geochim. Cosmochim. Acta. 75, 6048-6063.

Levasseur, S., Frank, M., Hein, J.R., Halliday, A., 2004. The global variation in the iron isotope composition of marine hydrogenetic ferromanganese deposits: implications for seawater chemistry? Earth Planet. Sci. Lett. 224, 91-105.

Manceau, A., Lanson, M., Geoffroy, N., 2007. Natural speciation of Ni, Zn, Ba, and As in ferromanganese coatings on quartz using X-ray fluorescence, absorption, and diffraction. Geochim. Cosmochim. Acta. 71, 95-128.

Maréchal, C.N., Nicolas, E., Douchet, C., Albarède, F., 2000. Abundance of zinc isotopes as a marine biogeochemical tracer. Geochem. Geophys. Geosyst. 1, 1-15.

Matthews, A.D., Riley, J.P., 1969. The determination of thallium in silicate rocks, marine sediments and sea water. Anal. Chim. Acta 48, 25-34.

McGoldrick, P.J., Keays, R.R., Scott, B.B., 1979. Thallium - Sensitive Indicator of Rock-Seawater Interaction and of Sulfur Saturation of Silicate Melts. Geochim. Cosmochim. Acta. 43, 1303-1311.

Nielsen, S.G., Gannoun, A., Marnham, C., Burton, K.W., Halliday, A.N., Hein, J.R., 2011. New age for ferromanganese crust 109D-C and implications for isotopic records of lead, neodymium, hafnium, and thallium in the Pliocene Indian Ocean. Paleoceanography 26, PA2213, doi:2210.1029/2010PA002003.

29

725 Nielsen, S.G., Mar-Gerrison, S., Gannoun, A., LaRowe, D., Klemm, V., Halliday, A.N., Burton, K.W., Hein,
726   J.R., 2009a. Thallium isotope evidence for a permanent increase in marine organic carbon export in the
727   early Eocene. Earth Planet. Sci. Lett. 278, 297-307.
728 Nielsen, S.G., Rehkämper, M., 2011. Thallium isotopes and their application to problems in earth and
729   environmental science, in: Baskaran, M. (Ed.), Handbook of Environmental Isotope Geochemistry.
730   Springer, pp. 247-270.
731 Nielsen, S.G., Rehkämper, M., Baker, J., Halliday, A.N., 2004. The precise and accurate determination of
732   thallium isotope compositions and concentrations for water samples by MC-ICPMS. Chem. Geol. 204,
733   109-124.
734 Nielsen, S.G., Rehkämper, M., Brandon, A.D., Norman, M.D., Turner, S., O'Reilly, S.Y., 2007. Thallium
735   isotopes in Iceland and Azores lavas - Implications for the role of altered crust and mantle
736   geochemistry. Earth Planet. Sci. Lett. 264, 332-345.
737 Nielsen, S.G., Rehkämper, M., Norman, M.D., Halliday, A.N., Harrison, D., 2006a. Thallium isotopic evidence
738   for ferromanganese sediments in the mantle source of Hawaiian basalts. Nature 439, 314-317.
739 Nielsen, S.G., Rehkämper, M., Porcelli, D., Andersson, P.S., Halliday, A.N., Swarzenski, P.W., Latkoczy, C.,
740   Günther, D., 2005. The thallium isotope composition of the upper continental crust and rivers - An
741   investigation of the continental sources of dissolved marine thallium. Geochim. Cosmochim. Acta 69,
742   2007-2019.
743 Nielsen, S.G., Rehkämper, M., Teagle, D.A.H., Alt, J.C., Butterfield, D., Halliday, A.N., 2006b. Hydrothermal
744   fluid fluxes calculated from the isotopic mass balance of thallium in the ocean crust. Earth Planet. Sci.
745   Lett. 251, 120-133.
746 Nielsen, S.G., Williams, H.M., Griffin, W.L., O'Reilly, S.Y., Pearson, N., Viljoen, F., 2009b. Thallium isotopes
747   as a potential tracer for the origin of cratonic eclogites. Geochim. Cosmochim. Acta. 73, 7387-7398.
748 Patterson, C.C., Settle, D.M., 1987. Magnitude of Lead Flux to the Atmosphere from Volcanos. Geochim.
749   Cosmochim. Acta. 51, 675-681.
750 Paytan, A., Kastner, M., Campbell, D., Thiemens, M.H., 1998. Sulfur isotopic composition of Cenozoic seawater
751   sulfate. Science 282, 1459-1462.
752 Peacock, C.L., Moon, E.M., 2012. Oxidative scavenging of thallium by birnessite: Controls on thallium sorption
753   and stable isotope fractionation in marine ferromanganese precipitates. Geochim. Cosmochim. Acta. 84,
754   297-313.
755 Prytulak, J., Nielsen, S.G., Plank, T., Barker, M., Elliott, T., 2013. Assessing the utility of thallium and thallium
756   isotopes for tracing subduction zone inputs to the Mariana arc. Chem. Geol. 345, 139-149.
757 Rehkämper, M., Frank, M., Hein, J.R., Halliday, A., 2004. Cenozoic marine geochemistry of thallium deduced
758   from isotopic studies of ferromanganese crusts and pelagic sediments. Earth Planet. Sci. Lett. 219, 77-
759   91.
760 Rehkämper, M., Frank, M., Hein, J.R., Porcelli, D., Halliday, A., Ingri, J., Liebetrau, V., 2002. Thallium isotope
761   variations in seawater and hydrogenetic, diagenetic, and hydrothermal ferromanganese deposits. Earth
762   Planet. Sci. Lett. 197, 65-81.
763 Rehkämper, M., Halliday, A.N., 1999. The precise measurement of Tl isotopic compositions by MC- ICPMS:
764   Application to the analysis of geological materials and meteorites. Geochim. Cosmochim. Acta. 63,
765   935-944.
766 Rehkämper, M., Nielsen, S.G., 2004. The mass balance of dissolved thallium in the oceans. Mar. Chem. 85, 125-
767   139.
768 Rudnick, R.L., Gao, S., 2003. Composition of the Continental Crust, in: Holland, H.D., Turekian, K.K. (Eds.),
769   Treatise on Geochemistry. Pergamon, Oxford, pp. 1-64.
770 Schauble, E.A., 2007. Role of nuclear volume in driving equilibrium stable isotope fractionation of mercury,
771   thallium, and other very heavy elements. Geochim. Cosmochim. Acta. 71, 2170-2189.
772 Schmitt, A.D., Galer, S.J.G., Abouchami, W., 2009. Mass-dependent cadmium isotopic variations in nature with
773   emphasis on the marine environment. Earth Planet. Sci. Lett. 277, 262-272.
774 Shaw, D.M., 1952. The geochemistry of thallium. Geochim. Cosmochim. Acta. 2, 118-154.
775 Siebert, C., Nägler, T.F., von Blanckenburg, F., Kramers, J.D., 2003. Molybdenum isotope records as a potential
776   new proxy for paleoceanography. Earth Planet. Sci. Lett. 211, 159-171.
777 Wasylenki, L.E., Rolfe, B.A., Weeks, C.L., Spiro, T.G., Anbar, A.D., 2008. Experimental investigation of the
778   effects of temperature and ionic strength on Mo isotope fractionation during adsorption to manganese
779   oxides. Geochim. Cosmochim. Acta. 72, 5997-6005.
780 Webb, S.M., Tebo, B.M., Bargar, J.R., 2005. Structural characterization of biogenic Mn oxides produced in
781   seawater by the marine bacillus sp strain SG-1. American Mineralogist 90, 1342-1357.
782 Wedepohl, K.H., 1974. Handbook of Geochemistry. Springer.
783 Zachos, J., Pagani, M., Sloan, L., Thomas, E., Billups, K., 2001. Trends, rhythms, and aberrations in global
784   climate 65 Ma to present. Science 292, 686-693.

785   Zachos, J.C., Dickens, G.R., Zeebe, R.E., 2008. An early Cenozoic perspective on greenhouse warming and
786   carbon-cycle dynamics. Nature 451, 279-283.
787
788
789

790

Figure Captions

Fig. 1. Plot of ε^{205}Tl vs. Tl concentration (note logarithmic scale) for various types of marine Fe-Mn deposits (Rehkämper et al., 2002). The dark and light shaded fields denote the Tl isotope compositions of hydrothermal fluids and seawater, which are characterized by ε^{205}Tl of -5.7 ± 0.4 and about -2.0 ± 0.5, respectively (Nielsen et al., 2004; Nielsen et al., 2006b; Rehkämper et al., 2002).

Fig. 2. Plot of the high-resolution ε^{205}Tl record obtained for two Fe-Mn crusts from the Pacific Ocean for the Cenozoic (Nielsen et al., 2009a). Shown for comparison are (at the top) the seawater S isotope record from marine barites (Kurtz et al., 2003; Paytan et al., 1998) and (at the bottom) the deep-sea oxygen isotope record from analyses of benthic foraminifera (Zachos et al., 2001; Zachos et al., 2008).

Fig. 3. (a) Thallium isotope compositions of recovered fluids and solids from time series experiments as a function of experimental duration, in terms of epsilon units, measured relative to NIST 997. (b) Thallium isotope fractionation factors between sorbed and dissolved Tl as a function of experiment duration. There is a small discernible increase in isotope fractionation during the first ~24 hr, after which no change is observed.

Fig. 4. (a) Fractionation factors for temperature and time series experiments, shown as a function of the fraction of Tl associated with the solid phase. Symbols are defined in the legend. (b) Fractionation factors for the same experiments as a function of μg Tl per mg birnessite.

Fig. 5. Thallium isotope fractionation factors between dissolved and solid Tl plotted versus the amount of Tl sorbed per milligram of birnessite. Also shown are hydrogenetic crust data from Rehkämper et al. (2002) and best-fit mixing lines for strongly fractionated and slightly fractionated Tl in two different sorbed sites. See text for details.

Fig. 6. Thallium isotope fractionation (α) between dissolved and solid Tl plotted versus the inverse of initial aqueous Tl concentration for low-Tl experiments.

823   Table 1: Experimental parameters for variable time and temperature adsorption experiments.

Experiment	Temp (°C)	Duration (hr)	Tl stock[*] (g)	MnO$_2$ stock (g)	H$_2$O (g)	[Tl] start sol. (μg/g)
Tl-3min	22	0.05	25.88	1.93	17.52	28.3
Tl-10min	22	0.16	25.19	2.00	18.11	27.6
Tl-6hr	22	6	24.59	2.00	18.35	27.1
Tl-24hr	22	24	25.50	1.97	17.77	28.0
Tl-48hr	22	48	25.41	1.97	18.02	27.8
Tl-72hr	22	72	25.25	1.98	17.87	27.8
Tl-6-04	6	50	4.92	0.51	4.36	24.9
Tl-6-05	6	50	4.94	0.25	4.62	25.0
Tl-6-06	6	50	2.98	1.01	1.98	24.8
Tl-25-01	25	48	10.37	1.99	8.17	25.1
Tl-25-02	25	48	10.27	1.00	9.13	25.0
Tl-25-03	25	48	10.46	0.50	9.61	25.2
Tl-25-04	25	48	10.75	0.25	9.95	25.5
Tl-40-01	40	2	3.06	0.97	2.01	25.1
Tl-40-02	40	2	5.09	0.51	4.53	24.9
Tl-40-03	40	2	5.09	0.25	4.87	24.7
LowTl-2201	22	44	0.247[†]	0.50	14.37[§]	0.464
LowTl-2202	22	44	0.251[†]	0.50	24.46[§]	0.277
LowTl-2203	22	44	0.250[†]	0.50	34.52[§]	0.195
LowTl-2204	22	44	0.248[†]	0.50	44.57[§]	0.150

824   [*]Stock solution had a Tl concentration of 49.6 μg/g, $\varepsilon^{205/203}$Tl = -0.3±0.3 (2sd), and 0.1 m KNO$_3$
825   for all but the four low-Tl experiments.
826   [†]Tl stock solution had 27.0 μg/g and $\varepsilon^{205/203}$Tl = -0.6±0.3 (2sd), for the four low-[Tl] experiments,
827   with no KNO$_3$.
828   [§]A solution of 0.1 m KNO$_3$ was used instead of H$_2$O for the four low-Tl experiments.
829
830

831 Table 2. Thallium mass balance and isotopic compositions of varied time and temperature adsorption
832 experiments.

Experiment	Total Tl (μg)	Tl in solid (μg)	Tl recovery[*] (%)	μg Tl/mg birnessite	[Tl] end sol. (μg/g)	$\varepsilon^{205}Tl_{diss}$	$\varepsilon^{205}Tl_{sorb}$	$\alpha_{sorb-diss}$
Tl-3min	1284	612	88	418.3	11.5	-1.4	0.7	1.00021
Tl-10min	1249	673	90	414.6	10.0	-1.5	0.7	1.00022
Tl-5hr	1220	669	90	404.3	9.7	-1.6	0.8	1.00024
Tl-24hr	1265	674	89	404.7	10.1	-1.8	1.1	1.00029
Tl-48hr	1260	622	87	379.8	10.4	-1.8	1.3	1.00031
Tl-72hr	1252	681	89	397.4	9.7	-1.9	1.2	1.00031
Tl-6-04	244	89	87	266.7	12.7	-2.4	2.2	1.00046
Tl-6-05	245	50	87	328.1	16.6	-1.5	2.9	1.00045
Tl-6-06	148	115	91	155.5	3.2	-6.6	0.6	1.00072
Tl-25-01	514	324	96	206.9	8.2	-4.3	1.7	1.00060
Tl-25-02	509	195	92	260.8	13.5	-2.2	2.3	1.00045
Tl-25-03	519	105	90	344.2	17.7	-1.4	2.6	1.00040
Tl-25-04	533	51	92	453.2	20.9	-0.9	2.7	1.00036
Tl-40-01	152	113	90	163.2	3.8	-5.5	0.5	1.00061
Tl-40-02	252	85	84	279.0	12.6	-2.2	1.9	1.00041
Tl-40-03	252	51	85	301.3	16.0	-1.2	2.4	1.00036

833 *Computed by adding weighted isotopic compositions of recovered fluid and solid and subtracting
834 from Tl stock solution's isotopic composition. Minor loss of both solid and liquid occurred for
835 most experiments. See text for details.
836

837

838 Table 3: Thallium mass balance and isotopic compositions of experiments performed at low Tl
839 abundances.

Experiment	Total Tl (µg)	Tl in solid (µg)	Tl recov.* (%)	µg Tl/ mg birnessite	[Tl] end sol. (µg/g)	$\varepsilon^{205}Tl_{diss}$	$\varepsilon^{205}Tl_{sorb}$	$\alpha_{sorb\text{-}diss}$
LowTl-2201	6.67	5.32	80	17	0.00034	-10.6	-0.8	1.00098
LowTl-2202	6.78	4.71	70	17	0.00054	-12.4	-1.4	1.00110
LowTl-2203	6.73	6.43	96	17	0.00050	-13.8	-0.9	1.00129
LowTl-2204	6.68	5.25	79	17	0.00086	-15.2	-0.7	1.00145

840 *Computed by adding weighted isotopic compositions of recovered fluid and solid and subtracting
841 from Tl stock solution's isotopic composition. See text for details.

842

843

844
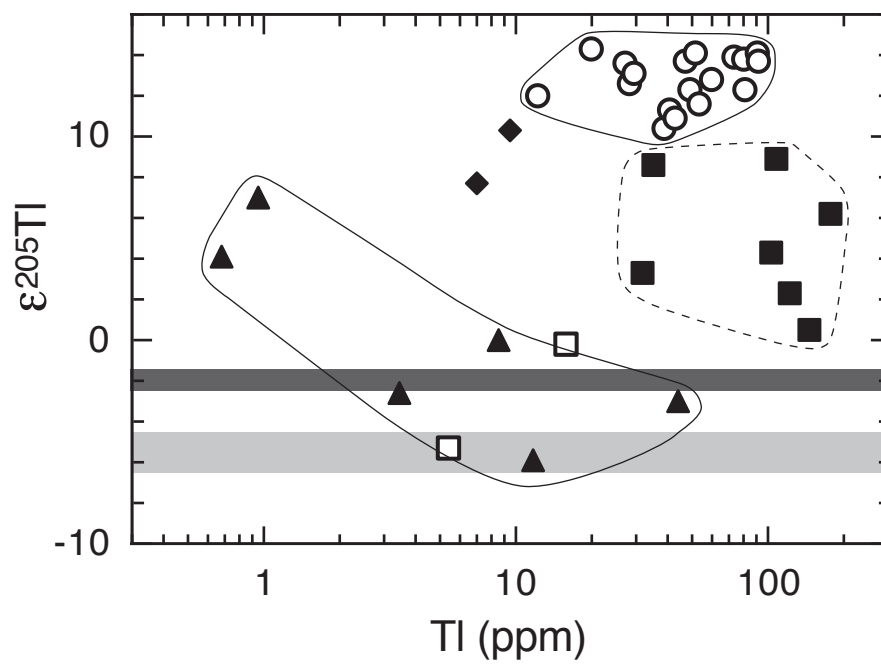
Fe-Mn Deposits:
○ Hydrogenetic
■ Diagenetic (deep-sea) □ Diagenetic (shallow-water)
▲ Hydrothermal ◆ Hydrothermal-hydrogenetic